

Investigation of Waypoint Characteristics for ZEM/ZEV Method for Moon Landing Problem

By
© 2022

Madison Sargent
B.S., University of Kansas, 2019

Submitted to the graduate degree program in Aerospace Engineering and the Graduate Faculty of the University of Kansas in partial fulfillment of the requirements for the degree of Master of Science.

Chair: Dr. Brian Kaplinger

Dr. Craig McLaughlin

Dr. Shawn Keshmiri

Date Defended: 19 January 2022

The thesis committee for Madison Sargent certifies that this is the approved version of the following thesis:

Investigation of Waypoint Characteristics for ZEM/ZEV Method for Moon Landing Problem

Co-Chair: Dr. Craig McLaughlin

Co-Chair: Dr. Shawn Keshmiri

Date Approved: 19 January 2022

Abstract

The focus of this research is to assess the use of waypoints and their effects on spacecraft guidance for a lunar landing scenario, using the Zero-Effort Miss/Zero-Effort Velocity (ZEM/ZEV) method. The lunar landing scenario simplifies equations and places the focus on the waypoint's effects. The goal of investigating using waypoints and how to evaluate them is to eventually provide the spacecraft guidance with a closed-loop solution that reduces computational demands in-flight and allow a spacecraft to compute an optimal path in-flight. By computing a path in-flight, mission fuel requirements related to path planning can be decreased, leading to significant savings across the industry. Other research in this area has not fully identified what parameters constitute a desirable waypoint and have typically chosen waypoints through a more brute force method. The solution to assess waypoint characteristics is to compute a path using the ZEM/ZEV method without a waypoint and then compare the path to a path with a single waypoint. When adding a single waypoint, characteristics are changed to see how much impact those characteristics have on the optimality of the path. Through these comparisons, it is found that the optimal path is not equivalent to a path with a waypoint inserted, regardless of what characteristic is changed. This shows that the ZEM/ZEV approach violates Bellman's principle of optimality because when the path is calculated from the waypoint to the final target, it does not result in the same trajectory for the remaining time. This suggests that the ZEM/ZEV approach, despite being proven as the optimal control law that satisfies the problem, may not have an optimal substructure. It is also found that gravity has a significant effect on the outcome of an optimal path and that when gravity is removed, the path with a waypoint is much closer to the optimal path.

Acknowledgments

I would like to acknowledge all the professors who have helped me throughout my career at KU. Their patience and guidance are what truly made the difference. I would also like to thank Dr. Kaplinger for his time and effort in helping with this thesis, as it would not have been possible without him. I would also like to thank family and friends that supported and encouraged me when I needed it the most. To my significant other, thank you for always being by my side and going through aerospace with me and having fun along the way.

I dedicate this thesis to my dog, Bella.

Table of Contents

1	Introduction.....	1
2	Background.....	5
3	Mathematical Model.....	13
3.1	ZEM/ZEV Equations.....	13
3.2	Genetic Algorithm.....	15
4	Numerical Simulations.....	17
4.1	ZEM/ZEV Method and Test Driver.....	17
4.2	Genetic Algorithm.....	31
5	Conclusion.....	36
6	References.....	39

List of Figures

Figure 1: General GNC Architecture	3
Figure 2. Apollo Explicit Guidance Method (Klumpp).....	6
Figure 3. Apollo Guidance Algorithms (Klumpp).....	7
Figure 4: ZEM/ZEV Path Without Waypoint Constraints (Guo, Hawkins and Wie, Waypoint-Optimized Zero-Effort-Miss/Zero-Effort-Velocity Feedback Guidance for Mars Landing)	9
Figure 5: ZEM/ZEV Path with Waypoint Optimization (Guo, Hawkins and Wie, Waypoint-Optimized Zero-Effort-Miss/Zero-Effort-Velocity Feedback Guidance for Mars Landing)	9
Figure 6: Optimal Path Using ZEM/ZEV Method Without a Waypoint.....	18
Figure 7: Comparison of Position for Optimal Path and Path with a Waypoint at 10%	20
Figure 8: Comparison of Position for Optimal Path and Path with a Waypoint at 50%	21
Figure 9: Comparison of Position for Optimal Path and Path with a Waypoint at 80%	21
Figure 10: Total Acceleration Across Time of Flight for Waypoint at 10%	23
Figure 11: Total Acceleration Across Time of Flight for Waypoint at 50%	23
Figure 12: Total Acceleration Across Time of Flight for Waypoint at 80%	24
Figure 13: Comparison of Position for Optimal Path and Path with a Waypoint at 10% with No Gravity	30
Figure 14: Fitness for GA at Final Generation	32
Figure 15: Position in X and Y for Genetic Algorithm (Population Size: 10000, Waypoint range: [6,99] sec)	33
Figure 16: Position in X and Y for Genetic Algorithm (Population Size: 1000, Waypoint range: [20,99] sec)	34

List of Tables

Table 1: Comparison of Total Acceleration from Different Path Configurations Pulled Off	
Original Optimal Path.....	22
Table 2: Comparison of Total Acceleration for Adjusted X Position for Waypoint Pulled Off	
Optimal Path	25
Table 3: Comparison of Total Acceleration for Adjusted Y Position for Waypoint Pulled Off	
Optimal Path	26
Table 4: Comparison of Different X Position Values for a Waypoint	27
Table 5: Comparison of Different Y Position Values for a Waypoint	27
Table 6: Comparison of Different X Velocity Values for a Waypoint.....	28
Table 7: Comparison of Different Y Velocity Values for a Waypoint.....	28
Table 8: Comparing Switching Time for a Path with a Waypoint at 50%	29
Table 9: Genetic Algorithm Results with Different Population Sizes	31
Table 10: Effects of Changing Waypoint Bounds for GA.....	35

1 Introduction

The space industry is interested in lunar missions again. Countries such as China, India, and the United States are attempting to return to the surface of the Moon. Reasons for this interest is the discovery of water and it being a potential source for astronaut consumption or rocket propellant, which could allow the Moon to become a gateway for missions that plan to travel further beyond (Chang). Other missions are also interested in learning more about the Moon's history and composition, which can teach us more about the early solar system. NASA has recently selected SpaceX to continue to develop Starship to take the next American astronauts to the Moon's surface as a part of the Artemis lunar program (NASA, As Artemis Moves Forward, NASA Picks SpaceX to Land Next Americans on Moon). The Artemis program aims to land the first woman and first person of color on the Moon to explore more of the lunar surface through new instrumentation and experiments. The first Commercial Lunar Payload Services (CLPS) will deliver 16 new instruments to the lunar surface, which include investigating the lunar polar soil and performing applied science and technology demonstrations in different locations on the Moon (NASA, The Artemis Plan). These instruments and experiments which will help to inform future deliveries to the Moon to make the possibility of having the Moon become a spaceport a reality.

China and India have also been active with their return to the Moon. In 2019, China landed a probe on the far side of the Moon and put the Yutu-2 rover to explore the Von Kármán crater during the Chang'e 4 mission (Society). A year later in 2020, China's Chang'e 5 mission sent a spacecraft that collected 3.82 lbs of sample near Mons Rümker, a volcanic feature (Jones). The samples collected by China were returned to Earth, making them the first samples collected since the Soviet Union's 1976 Luna 24 mission (Myers). India has been launching missions with

the intention of having a lunar lander. Their recent mission, Chandrayaan-2 began its' lunar orbit in 2019 and attempted to deploy a lunar lander but was unsuccessful. However, the Indian Space Research Organization (ISRO) has approved Chandrayaan-3, which will attempt to deploy a moon lander and rover to the surface of the Moon in 2022 (Singh). India's intentions with these missions are to demonstrate capability to land and eventually perform interplanetary missions.

With this newfound interest in returning, researching, and utilizing the Moon, it is important that missions become more sustainable, efficient, and autonomous, which will allow visits to the Moon to become more frequent. One way to do this is by improving the guidance portion of the guidance, navigation, and control (GNC) that a spacecraft uses. Guidance is applicable to different mission phases, such as ascent, on-orbit, rendezvous, planetary approach, and landing. A typical GNC loop is seen in Figure 1, where the guidance is open-loop, indicating that it cannot adapt to what is actually happening. A common guidance method for spacecraft is to compute optimal trajectory to a landing target offline, which is computationally expensive and unfeasible in flight. This type of guidance was commonly used with intercontinental ballistic missiles (Siouris). A fundamental issue with this type of guidance is that it does not reflect the current conditions of the spacecraft and if it is still travelling along an optimal path. If some external disturbance, mechanism failure or other disruption displaces the spacecraft off the optimal path, then it would not have the capability to update and create a new optimal path; instead, it would attempt to go back to and continue the original optimal path. The issue with this is the path having been calculated offline may no longer be the optimal path for the spacecraft to follow and the spacecraft has now wasted valuable fuel resources to follow that path.

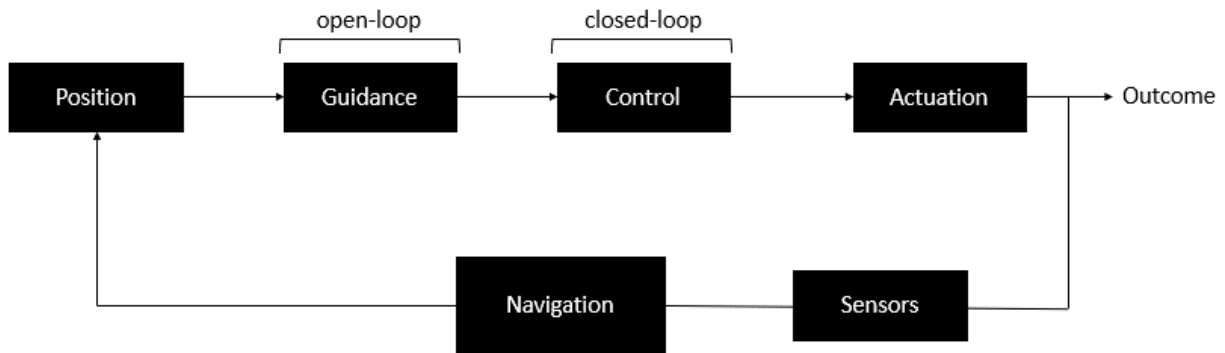


Figure 1: General GNC Architecture

One method to solve this issue is to focus on computing the trajectory online in specific time increments. If the spacecraft is focusing on the optimal solution for the next ten seconds, for example, then it will always follow along an optimal path. However, for this to be successful, it is important to know how a good waypoint is chosen. There are certain factors that can be changed, assessed, and then compared to the optimal path to determine if a method of adding waypoints can still compute an optimal path or close to it with minimal computational power. There is optimization software that exists to find the best waypoint, but this requires more computation power and does not fundamentally explain what characteristics are being optimized.

To implement the use of waypoints, a zero-effort-miss/zero-effort-velocity (ZEM/ZEV) guidance method can be used, which is an extension of optimal guidance laws. ZEM is the *distance* that a spacecraft misses the target if no further accelerations are made, after a certain time, t while ZEV is the *velocity* error at the end of the mission if no further accelerations are made after a certain time, t . ZEM has historically been used for ballistic missile problems and it was Ebrahimi et al. who further advanced the concept to also include ZEV (Ebrahimi, Bahrami

and Roshanian). The use of ZEV can typically be categorized as successful if the ZEV error outcome is zero if a mission has a required final velocity. For planetary landing missions, the final velocity is typically zero. This is also the case for rendezvous missions.

2 Background

The modern trajectory optimization that is seen today was originally explored by Oberth, Hohmann, and Goddard (Oberth; Hohmann; Goddard) . The history of early trajectory optimization between 1950-1963 is detailed by Lawden (Lawden). Different versions of GNC have been used to achieve mission goals, such as with Apollo missions. According to a report written by Allan Klumpp on Apollo Guidance, Navigation, and Control, there are two ways to guide a spacecraft to a current state to a specified target state, either implicitly or explicitly. While it is unclear what each Apollo landing mission did (Apollo 11, 12, 14, 15, 16, and 17), Klumpp indicates in the paper that implicit guidance had not been developed when Apollo 11 was coded and that although there were advantages to an implicit method, they were not enough to warrant recoding guidance for later missions (Klumpp). This indicates that the explicit method was used. The explicit method is when you repeat calculations as the mission progresses to find a vector polynomial function that intersects between the current and target state. Once that is found, the guidance method can then command a profile of acceleration vs. time. The explicit method is less robust to deviations that can occur in flight, and so is more affected by control errors. The equation shown in Figure 2 is the final explicit guidance equation used on Apollo, which is corrected to consider when to command an acceleration, where ACG is the commanded acceleration, RTG is the target position, RG is the current position, VTG is the target velocity, VG is the current velocity, and ATG is the target acceleration. The variables for time are T_P and T , where T_P is the predicted target reference time, which is the sum of the current time, T , and the leadtime, which is the delay that occurs from performing computation and command.

$$\begin{aligned}
 \underline{ACG} = & \left[3 \left(\frac{T_P}{T} \right)^2 - 2 \left(\frac{T_P}{T} \right) \right] 12 (\underline{RTG} - \underline{RG})/T^2 + \left[4 \left(\frac{T_P}{T} \right)^2 - 3 \left(\frac{T_P}{T} \right) \right] 6 \underline{VTG}/T \\
 & + \left[2 \left(\frac{T_P}{T} \right)^2 - \left(\frac{T_P}{T} \right) \right] 6 \underline{VG}/T + \left[6 \left(\frac{T_P}{T} \right)^2 - 6 \left(\frac{T_P}{T} \right) + 1 \right] \underline{ATG}.
 \end{aligned} \tag{11}$$

Figure 2. Apollo Explicit Guidance Method (Klumpp)

During Apollo, although there was a designated landing site, it was still possible to redesignate the landing site while in-flight. Each time this is done, the guidance algorithm is rerun to compute a new thrust-acceleration command for the lander, and this continues until the lander is safely on the surface. The full algorithm, designated as P63 and P64 is shown in Figure 3.

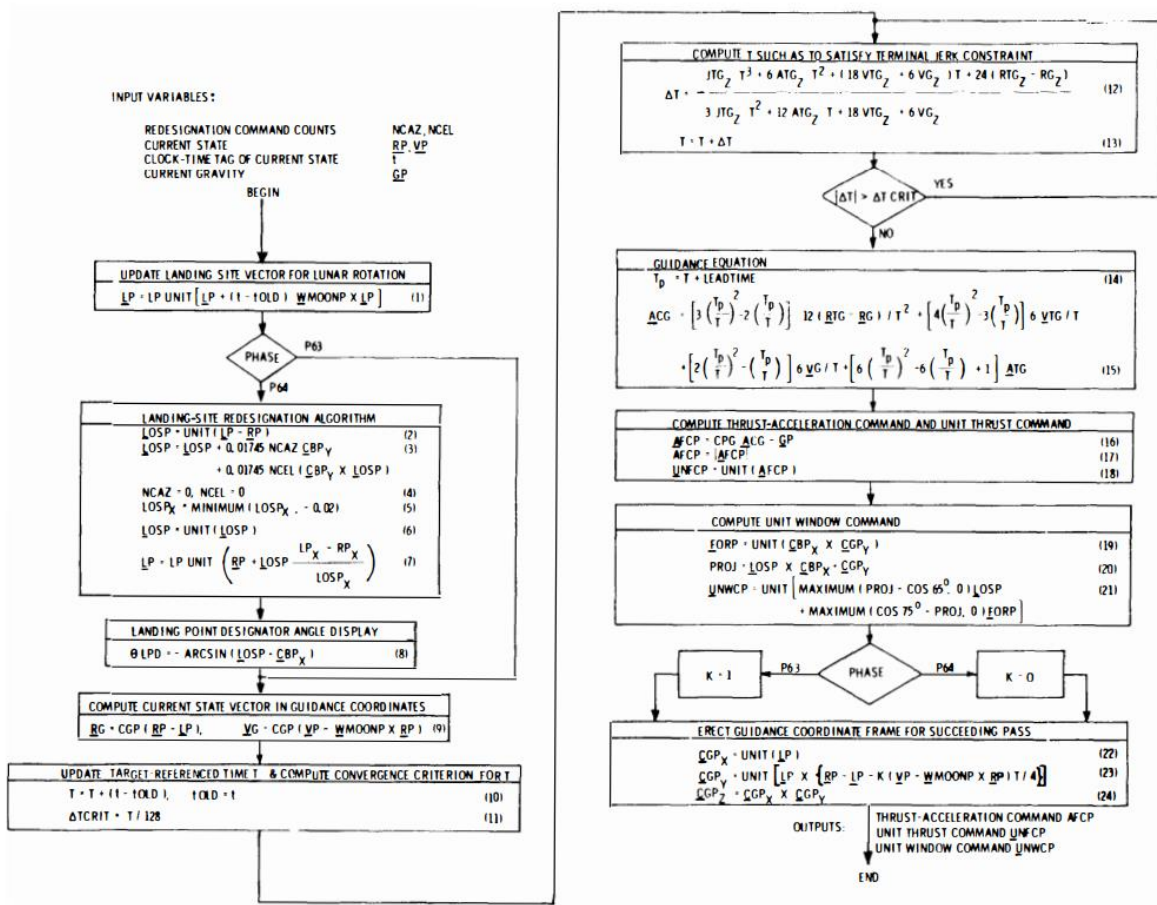


Figure 6 P63, P64 Guidance Algorithm

Figure 3. Apollo Guidance Algorithms (Klump)

The research in optimal control theory spans several aerospace applications such as planetary landing, rendezvous and docking, asteroid intercept, and ballistic missile intercept. Although the concept of zero-effort-miss/zero-effort-velocity is newer, optimal control theory has been long used in aerospace applications (Bryson and Ho; Ben-Asher). It is important to note that ZEM/ZEV is not always an optimal solution, but Guo et al. showed in an environment with uniform gravitation, it is (Guo, Hawkins and Wie, Applications of Generalized Zero-Effort-Miss/Zero-Effort-Velocity Feedback Guidance Algorithm). Prior to Guo, et al., D’Souza had

explored the use of an optimal control algorithm in a uniform field for a planetary landing (D'Souza). Bong Wie introduced the idea of a waypoint optimized ZEM/ZEV path using a waypoint as an intermediate target to avoid lander collision during a planetary landing (Wie). Sharma et al. also considered the waypoint concept to investigate solving optimal control problems that are nonlinear and have terminal constraints (Sharma, Hurtado and Vadali).

Improving on previous guidance algorithms allows for less error and therefore less accelerations needed in flight. There have been different modifications to the ZEM/ZEV method, to improve it for specific applications. Waypoint optimized ZEM/ZEV for a Mars landing problem has shown results close to optimal performance, while still having the benefits of feedback control. Guo et al. performed a study of using a waypoint as an intermediate target and discovered that using only one waypoint allows for close to optimal flight performance (Guo, Hawkins and Wie, Waypoint-Optimized Zero-Effort-Miss/Zero-Effort-Velocity Feedback Guidance for Mars Landing). Figure 4 and Figure 5 shows how implementing the waypoint allows for the no subsurface flight constraint to be achieved. However, the research done by Guo et al. only chose a waypoint by using trial and error methods until their desired outcome was achieved. In the paper, Guo et al. state that further research is needed to develop, “real-time computation of the optimal waypoint” (Guo, Hawkins and Wie, Waypoint-Optimized Zero-Effort-Miss/Zero-Effort-Velocity Feedback Guidance for Mars Landing).

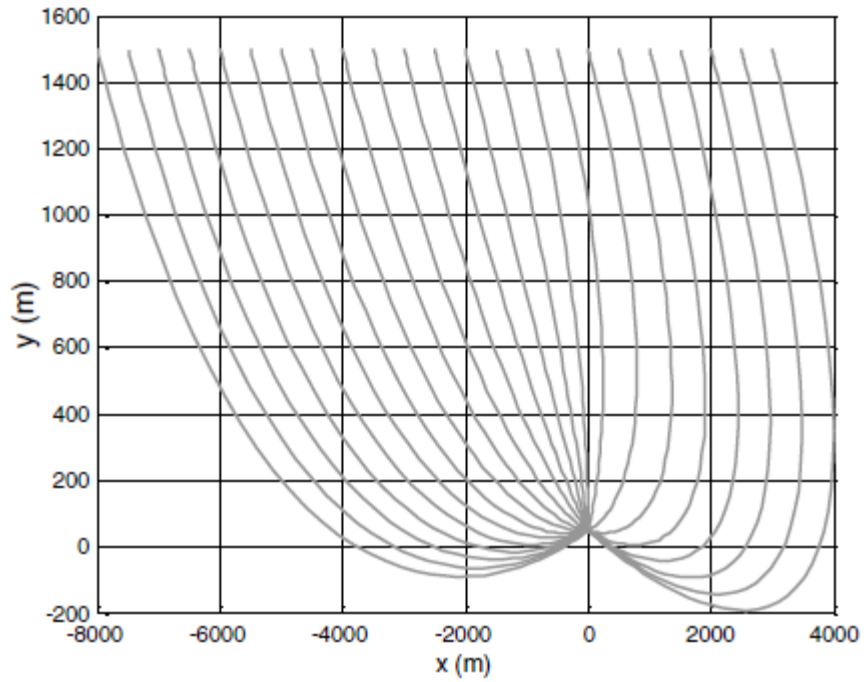


Figure 4: ZEM/ZEV Path Without Waypoint Constraints (Guo, Hawkins and Wie, Waypoint-Optimized Zero-Effort-Miss/Zero-Effort-Velocity Feedback Guidance for Mars Landing)

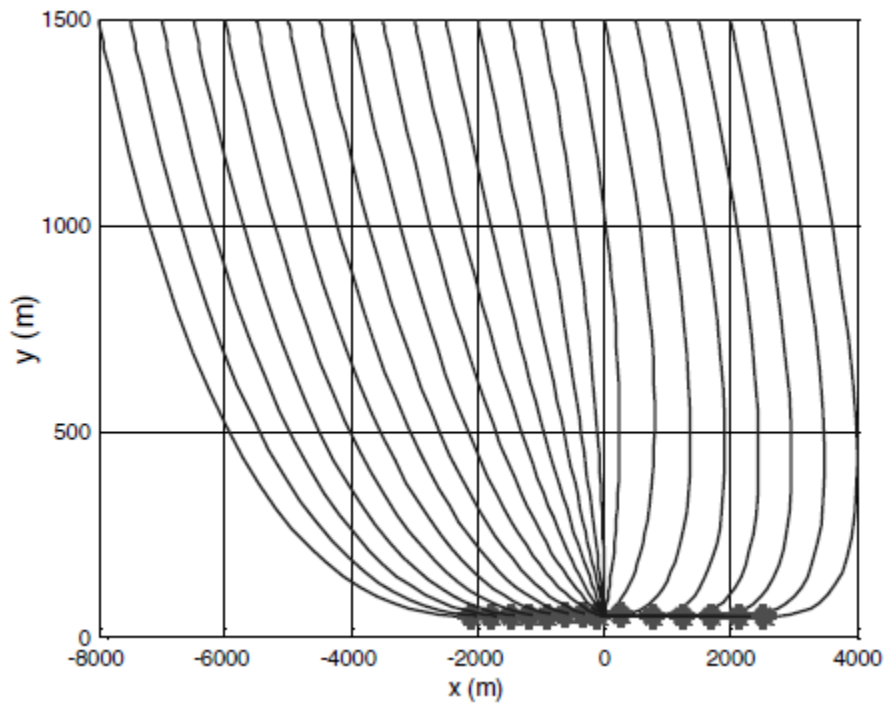


Figure 5: ZEM/ZEV Path with Waypoint Optimization (Guo, Hawkins and Wie, Waypoint-Optimized Zero-Effort-Miss/Zero-Effort-Velocity Feedback Guidance for Mars Landing)

In Guo et al's paper *Optimized Zero-Effort-Miss/Zero-Effort-Velocity Feedback Guidance for Mars Landing*, it is said that the method for choosing a waypoint is through trial and error. The research presented in this thesis attempts to move away from trial and error by exploring waypoint characteristics to determine how a good waypoint can be chosen. This eliminates the trial and error process and aims to provide a clear method for choosing a waypoint.

The PhD dissertation of Matt Hawkins further explored the use of waypoints as an intermediate target for a Mars landing problem. Hawkins focuses more on selecting a specific waypoint time and chooses to use a waypoint time corresponding to the minimum altitude across the mission time. Hawkins also explores two different versions of a waypoint-optimized ZEM/ZEV method. The first version focuses on enforcing a no-subsurface flight constraint, while the second version focuses on maintaining a glide slope above four degrees while using a waypoint. When Hawkins compares the original ZEM/ZEV method to the waypoint optimized ZEM/ZEV paths, it is shown that the fuel usage of the waypoint-optimized schemes to the original ZEM/ZEV method are extremely close, with the waypoint path with a no subsurface constraint being almost identical to the original ZEM/ZEV path without a waypoint and the waypoint path with a glide slope constraint needing only slightly more fuel than the original ZEM/ZEV path (Hawkins). Hawkins also compared adjusting the ZEM/ZEV method time of flight to satisfy no subsurface constraints and found that when using the waypoint optimized method to avoid subsurface flight, it outperforms simply adjusting the time of flight for the ZEM/ZEV method. In fact, the waypoint optimized ZEM/ZEV method not only satisfies the no subsurface constraint, but also achieves close to optimal performance. These results come from the work focused on a power-limited engine, but Hawkins also does explore a thrust-limited engine.

While Hawkins does explore the use of waypoints in a landing problem and focuses on optimization, the waypoints in these instances are found using optimization software. The waypoint optimization problem is solved through using software that solves a standard quadratic programming problem. Using optimization software gives an optimal waypoint, but does not allow for understanding why that specific waypoint is optimal. The research in this thesis is exploring the individual characteristics of a waypoint to understand what can make a waypoint an optimal waypoint, as opposed to a software producing it.

The thesis of Armando Alvarez Rolins also explores using a single waypoint driven trajectory, but for a rendezvous with a rotating target. The goal of Alvarez Rolins using a waypoint is to avoid collision with the rotating target. While Alvarez Rolins does explore the use of LQR, Mixed, and ZEM/ZEV methods with a waypoint, for the purpose of this research, only the results of the ZEM/ZEV methods with a waypoint will be discussed (Alvarez Rolins). While implementing the waypoint constraint does increase cost, it also avoids collision with the target, which is of primary importance. Alvarez Rolins investigated which combination of using a waypoint would yield the least added cost. Alvarez Rolins finds that for a rendezvous with a rotating target, a single waypoint implemented toward the later portion of the flight avoids collision and is less cost than a waypoint implemented in the earlier flight time.

Alvarez Rolins chooses the waypoint based on a certain percentage of flight. This does provide some insight and is more informative than brute trial and error, but Alvarez Rolins stops there. Only the metric of percentage of flight is used to choose the waypoint and it does not provide a global answer for choosing an optimal waypoint. It is important to note that the method of a waypoint as a percentage of the flight time is explored as part of the thesis presented here, but the primary difference is that it is only one test case in the process of examining an optimal

waypoint's characteristics. Several other characteristics are examined and presented later in the research to determine an optimal waypoint's characteristics.

3 Mathematical Model

3.1 ZEM/ZEV Equations

The main mathematical model that is focused on in this research is the ZEM/ZEV feedback guidance. The zero-effort miss (ZEM) is the position at the end if no further acceleration is applied, while the zero-effort velocity (ZEV) is the velocity at the end if no further acceleration is applied. This numerical setup is for finding a path with a waypoint. This is because the research focuses on calculating new paths when an external disturbance or mechanism failure causes a spacecraft to be offset from the original desired path. The use of waypoints allows the spacecraft to travel along a new path that still reaches the desired target, instead of wasting resources to travel back to the original path. The dynamic equations of motions for the spacecraft are

$$\dot{\mathbf{r}} = \mathbf{v} \quad (3.1)$$

$$\dot{\mathbf{v}} = \mathbf{g} + \mathbf{a} \quad (3.2)$$

where \mathbf{r} represents the position vector; \mathbf{v} represents the velocity vector; \mathbf{g} represents gravitational acceleration acting on the spacecraft; and \mathbf{a} represents the acceleration vector. Gravitational acceleration can be a function of position, but because this is a lunar landing mission, it remains constant with the Moon's gravity. Both \mathbf{r} and \mathbf{v} vectors are represented as 2x1 column vectors.

The boundary conditions for ZEM/ZEV are as follows

$$\begin{aligned} \mathbf{r}(t_0) = \mathbf{r}_0 \quad \mathbf{r}(t_f) = \mathbf{r}_t \\ \mathbf{v}(t_0) = \mathbf{v}_0 \quad \mathbf{v}(t_f) = \mathbf{v}_t \end{aligned} \quad (3.3)$$

where \mathbf{r}_0 and \mathbf{v}_0 are the initial position and velocity, respectively, while \mathbf{r}_t and \mathbf{v}_t are the target position and velocity, respectively and t_0 and t_f are initial and final time, respectively.

The formulation of the Hamiltonian below and subsequent equations is with respect to optimizing the objective function, J , which is

$$J = \frac{1}{2} \int_{t_0}^{t_f} \mathbf{a}^T \mathbf{a} dt \quad (3.4)$$

The Hamiltonian function is

$$H = \frac{1}{2} \mathbf{a}^T \mathbf{a} + \mathbf{p}_r^T \mathbf{v} + \mathbf{p}_v^T (\mathbf{g} + \mathbf{a}) \quad (3.5)$$

where \mathbf{p}_r is the costate vector associated with position and \mathbf{p}_v is the costate vector associated with velocity. The costate equations are then found by taking partial derivatives from Eq. 3.5, with respect to position, velocity, and acceleration. Once the costate equations are found, it is important to define the time-to-go. The time-to-go is calculated as follows

$$t_{go} = t_f - t_p \quad (3.6)$$

where t_f is final time and t_p is current time. The relation in Eq. 3.3 is used to make substitutions into the costate equations and further define the optimal control law as

$$\mathbf{p}_r = \mathbf{p}_r(t_f) \quad (3.7)$$

$$p_v = t_{go} \mathbf{p}_r(t_f) + \mathbf{p}_v(t_f) \quad (3.8)$$

$$\mathbf{a} = -t_{go} \mathbf{p}_r(t_f) - \mathbf{p}_v(t_f) \quad (3.9)$$

By substituting into the dynamic equations and then solving for \mathbf{p}_r and \mathbf{p}_v , the optimal control law can now be defined as

$$\mathbf{a} = \frac{6[\mathbf{r}_t - (\mathbf{r} + t_{go} \mathbf{v})]}{t_{go}^2} - \frac{2(\mathbf{v}_t - \mathbf{v})}{t_{go}} \quad (3.10)$$

The current position and current velocity can explicitly be defined as

$$\mathbf{r}_p = \mathbf{r} + t_{go}\mathbf{v} + \frac{1}{2}\mathbf{g}_{moon}(t_{go}^2) \quad (3.11)$$

$$\mathbf{v}_p = \mathbf{v} + \mathbf{g}_{moon}t_{go} \quad (3.12)$$

where \mathbf{r}_p is the current position; \mathbf{v}_p is the current velocity; \mathbf{g}_{moon} is the Moon's gravity; \mathbf{r} is the position vector; \mathbf{v} is the velocity vector and t_{go} is the time-to-go. The current position, current velocity, and Moon's gravity are 2x1 column vectors. Next, the ZEM and ZEV expressions are found with the following equations (Ebrahimi, Bahrami and Roshanian; Furfaro, Cupples and Cribb)

$$\mathbf{ZEM} = \mathbf{r}_t - \mathbf{r}_p \quad (3.13)$$

$$\mathbf{ZEV} = \mathbf{v}_t - \mathbf{v}_p \quad (3.14)$$

where \mathbf{r}_t is the target or final position and \mathbf{v}_t is the target or final velocity. By simplifying and substituting in Eq. 3.13 and 3.14, acceleration is then defined as the following equation (Guo, Hawkins and Wie, Optimal Feedback Guidance Algorithms for Planetary Landing and Asteroid Intercept; Braun and Manning)

$$\mathbf{a} = \frac{6}{t_{go}^2}\mathbf{ZEM} - \frac{2}{t_{go}}\mathbf{ZEV} - \mathbf{g} \quad (3.15)$$

where \mathbf{a} is a 2x1 column vector, comprised of the x and y components. The total acceleration is found by taking the norm of the acceleration vector components.

3.2 Genetic Algorithm

The genetic algorithm uses the equations in the test driver, which are 3.11 – 3.15. The only additional equation needed to assess the results of the genetic algorithm is the derivative between the ZEM/ZEV driver results and the genetic algorithm results. To find the derivative, the equation is

$$\frac{d_a}{d_x} = \frac{a_{ZEM-O} - a_{GA}}{x_{ZEM-O} - x_{GA}} \quad (3.16)$$

where a_{ZEM-O} and a_{GA} are the total acceleration values for the ZEM/ZEV optimal path (without a waypoint) and the genetic algorithm, respectively. The x_{ZEM-O} and the x_{GA} are the x positions for the ZEM/ZEV optimal path (without a waypoint) and the genetic algorithm, respectively.

4 Numerical Simulations

Simulations provide necessary insight to the problem being investigated. In this case, numerical results show quantitative differences between the optimal solution and a solution with a waypoint. Different types of numerical simulations, as well as iterations to specific simulations are utilized to try and identify what causes the optimal solution to differ from a solution with a waypoint.

Section 4.1 shows numerical results from the ZEM/ZEV method. First, the optimal path is calculated using the ZEM/ZEV method with no waypoint. Then, the same script is modified to include a waypoint that is chosen in one of two ways: 1.) A waypoint inserted at a certain percentage of the path, such as 50%, or 2.) An arbitrary waypoint defined by the x and y position, and the x and y velocity. The modified ZEM/ZEV method serves as the main test driver for the waypoint driven results.

4.1 ZEM/ZEV Method and Test Driver

The initial test driver used to compare the optimal path to a path with a waypoint is done using ode45 in Matlab, which calls a function that includes a traditional ZEM/ZEV method. The Matlab function ode45 solves ordinary differential equations (ODE) and uses the Runge-Kutta method to efficiently compute results. The ode45 function accepts the function or equation of interest and the initial conditions to solve the mathematical problem. The ZEM/ZEV method uses Eq. 3.6, 3.11 – 3.15 and has the boundary conditions defined in Eq. 3.3.

The input to the ZEM/ZEV function is the TOF and the target position and velocity. For this simulator, the time of flight (TOF) is consistently 100 seconds, with a target position, $\mathbf{r}_t = [0 \text{ m}, 0 \text{ m}]^T$ in the x and y directions, respectively and the target velocity, $\mathbf{v}_t = [0 \text{ m/s}, 0 \text{ m/s}]^T$ in the x and y directions, respectively. To simulate a Moon lander problem, the gravity of the

moon is applied to the ZEM/ZEV equations inside the function. The gravity of the moon is $[0, -1.62 \text{ m/s}^2]$, with the downward direction being the negative orientation. The input to the ode45 function is the range for TOF, starting at zero and incrementally increasing to the final TOF, as well as the initial position and velocity. The initial position is, $\mathbf{r}_0 = [-100\text{m}, 100\text{m}]^T$ in the x and y direction, respectively, while the initial velocity is, $\mathbf{v}_0 = [100\text{m/s}, -5\text{m/s}]^T$ in the x and y direction, respectively. Figure 6 shows the output for the optimal path using the ZEM/ZEV method without a waypoint. The green asterisk indicates the starting position of the path and the red asterisk indicates the end point of the path. The total acceleration this path requires is 216.9971 m/s^2 .

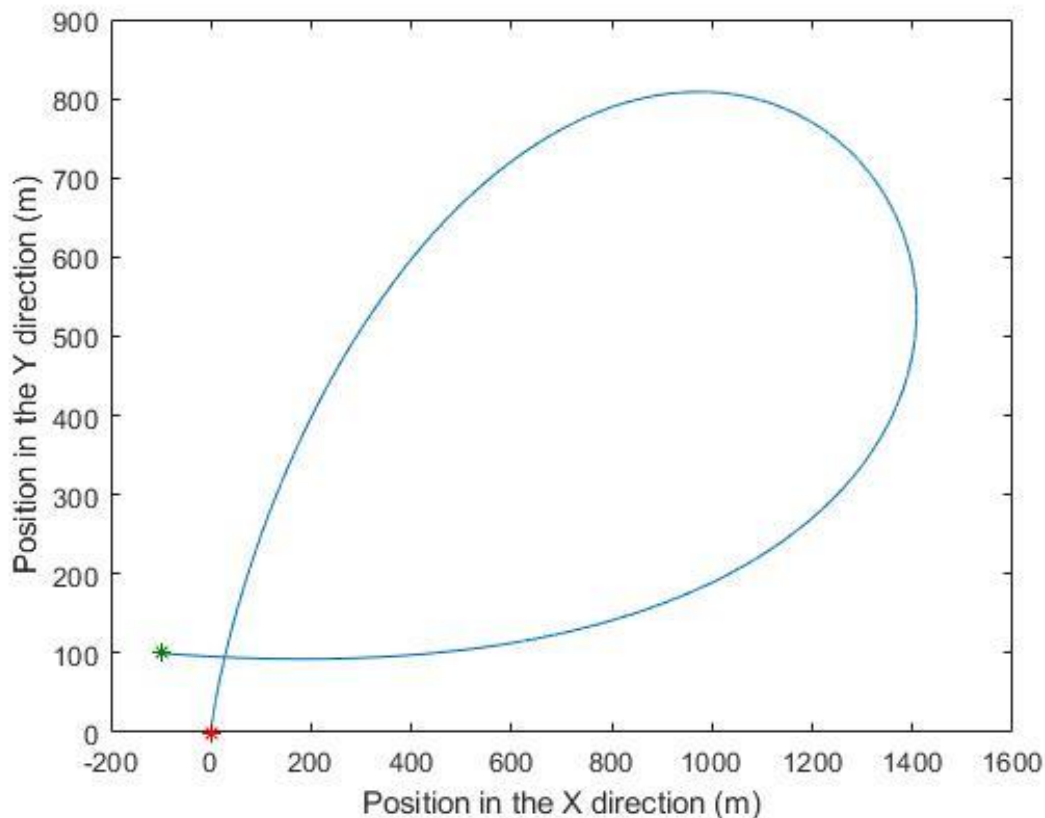


Figure 6: Optimal Path Using ZEM/ZEV Method Without a Waypoint

The simulated problem presented in this research and the use of waypoints is for recovering from an external disturbance or mechanism failure. The goal of calculating a new path after a disturbance has happened through using waypoints is to provide a path that takes less total acceleration than going back and following the original calculated path, which is now out of the way. By using a waypoint, the spacecraft can now start from a new initial position, but still achieve the same target position. There are two different methods that a waypoint is implemented with this test driver. The first method is inserting a waypoint onto the original optimal path at a certain percentage of that path. In this case, the waypoint characteristics (position in x and y, velocity in x and y, and waypoint time) are all specified as a percentage of the previously calculated optimal path. The second method is choosing an arbitrary waypoint by providing the position and velocity in the x and y direction, as well as the time of the waypoint. A main outcome of this test driver is the total acceleration that a path requires. Differences in total acceleration show which path requires more energy and the less energy required, the more optimal a path is. The total acceleration serves as a cost function for this research.

From testing percentages off the original optimal path, the results presented in Table 1 show that there is likely a minimum existing between a waypoint existing at 50% and a waypoint existing at 60%. This is because the acceleration for a path with a waypoint at 50% reaches a minimum value before starting to increase again for a path with a waypoint at 60%. Figure 7- Figure 9 show the position in the x and y direction plotted against the original optimal ZEM/ZEV path. Figure 8 is a representation of what the path with a waypoint and the lowest total acceleration looks like. The other paths with a waypoint essentially undershoot and overshoot this minimum acceleration. It also should be noted that the path with a waypoint at 50% shows less total acceleration needed than the original optimal ZEM/ZEV path. It also important that the

highest total acceleration for a path with a waypoint appears for the paths when the waypoint occurs later in the path, such as a path with a waypoint at 80% or 90%.

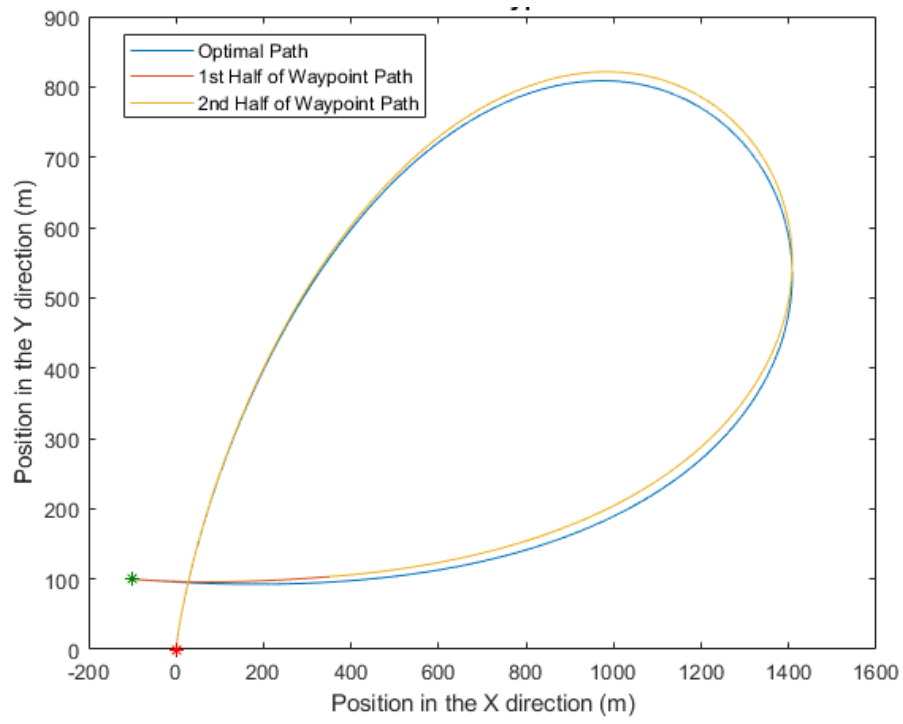


Figure 7: Comparison of Position for Optimal Path and Path with a Waypoint at 10%

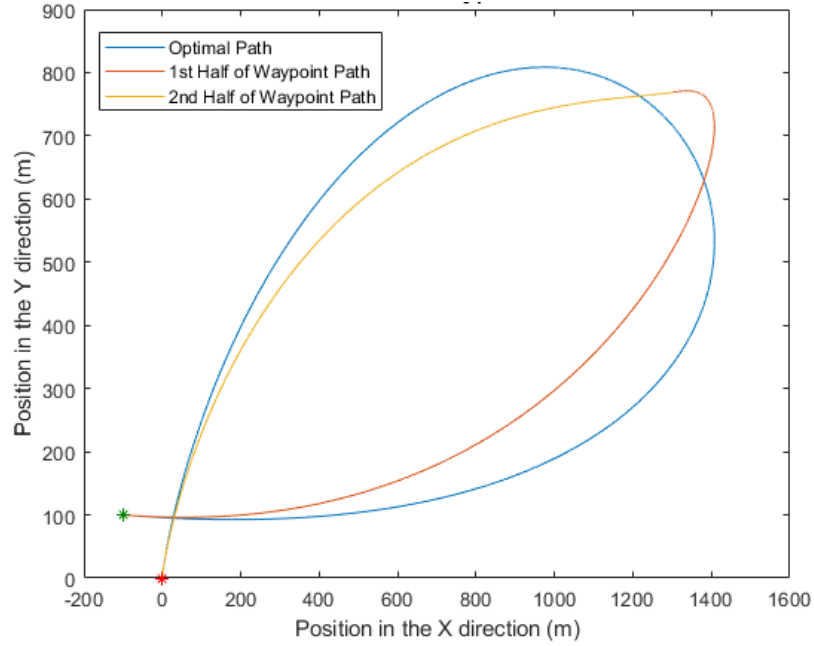


Figure 8: Comparison of Position for Optimal Path and Path with a Waypoint at 50%

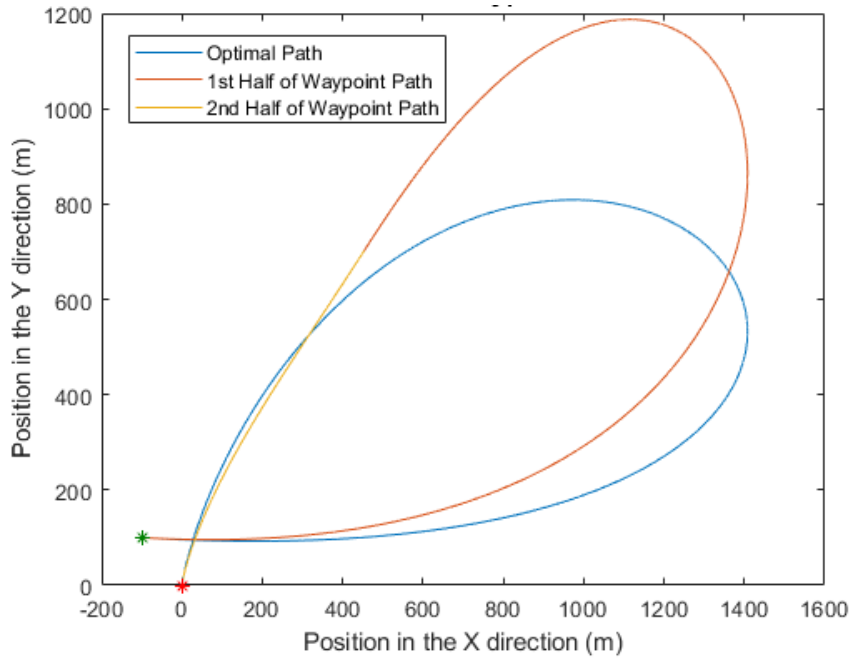


Figure 9: Comparison of Position for Optimal Path and Path with a Waypoint at 80%

Table 1: Comparison of Total Acceleration from Different Path Configurations Pulled Off Original Optimal Path

Path Description	Total Acceleration (m/s²)
Original optimal path	216.9971
Path with a waypoint at 10%	217.7369
Path with a waypoint at 20%	216.5945
Path with a waypoint at 30%	215.1787
Path with a waypoint at 40%	213.9899
Path with a waypoint at 50%	213.6398
Path with a waypoint at 60%	215.2954
Path with a waypoint at 70%	225.0829
Path with a waypoint at 80%	243.1986
Path with a waypoint at 90%	255.1346

As expected, when the acceleration throughout the entire TOF is plotted, in Figure 10 - Figure 12, the paths that have the most similar total acceleration to the original optimal path show the same trends throughout. For the paths when the total acceleration is less than the total acceleration for the original optimal path (i.e. paths with a waypoint at 50%), it shows trends of higher acceleration toward the midpoint of the path and then slightly lower toward the end. For the paths when the total acceleration is higher than the total acceleration for the original path (i.e. paths with a waypoint at 80%), the acceleration is highest toward the end of the path, indicating that for a planetary landing, having a waypoint at the end of the path requires more effort.

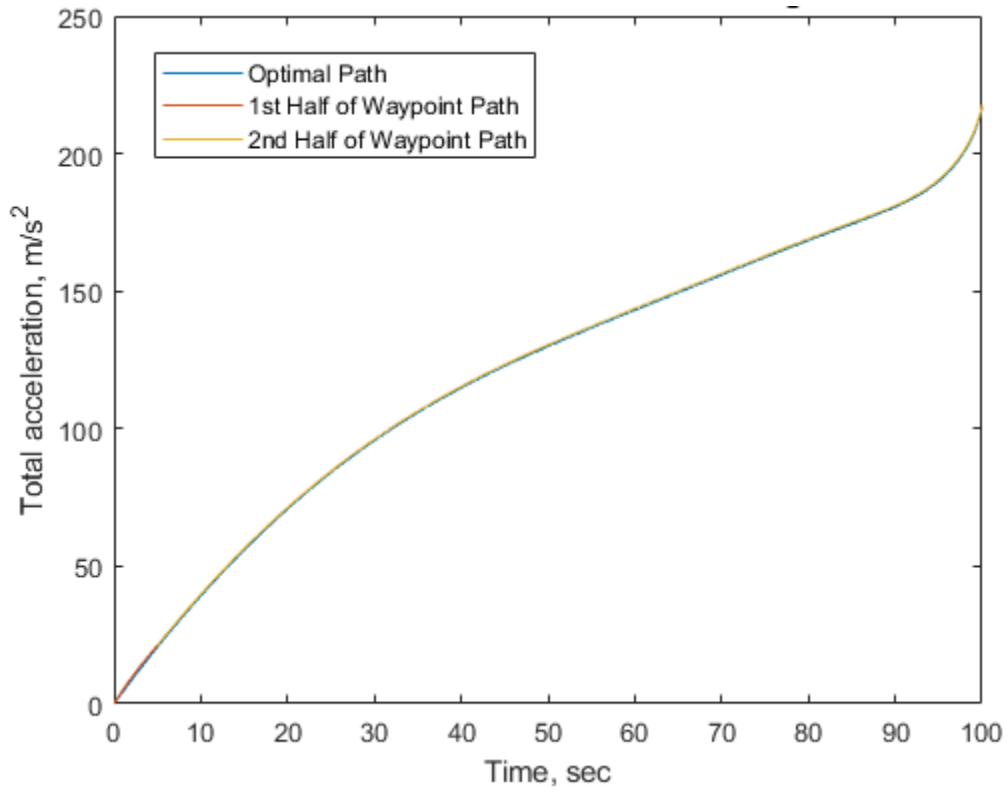


Figure 10: Total Acceleration Across Time of Flight for Waypoint at 10%

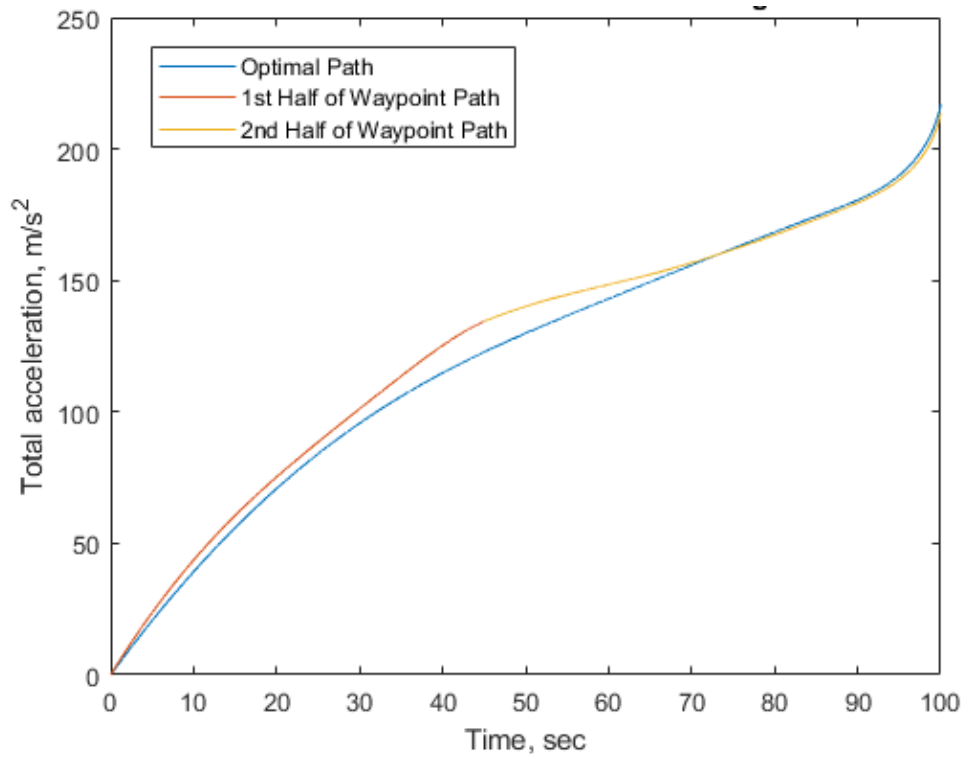


Figure 11: Total Acceleration Across Time of Flight for Waypoint at 50%

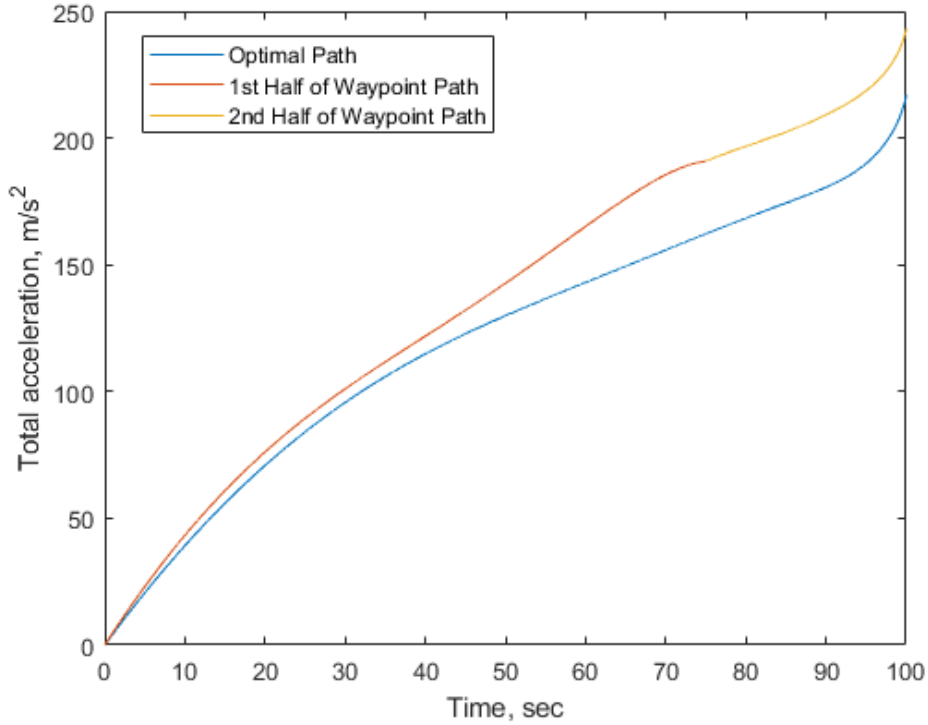


Figure 12: Total Acceleration Across Time of Flight for Waypoint at 80%

Small changes on a waypoint are also investigated. After a waypoint is inserted into the path, changes to the x and y position are applied. These changes are only applied to either the x position or the y position and are not applied simultaneously to both. This helps isolate the changes and allows a direct comparison between a path with a waypoint and a path with an adjusted waypoint position. Through altering the position, the derivative is found, which if the derivative is zero, it indicates a sign of an optimal solution. The equation to find the derivative is

$$\frac{d_a}{d_x} = \frac{a_{wp} - a_{wpa}}{x_{wp} - x_{wpa}} \quad (4.2)$$

where a_{wp} and a_{wpa} represent the acceleration for the path with a waypoint and the acceleration for a path with a waypoint that is adjusted, respectively; and x_{wp} and x_{wpa} represent the position in the x direction at the waypoint for the path with a waypoint and the position in the x direction

at the waypoint for a path with an adjusted waypoint. The other version of this equation adjusts the y position instead of the x position and is

$$\frac{d_a}{d_y} = \frac{a_{wp} - a_{wpa}}{y_{wp} - y_{wpa}} \quad (4.3)$$

where y_{wp} and y_{wpa} represent the position in the y direction at the waypoint for the path with a waypoint and the position in the y direction at the waypoint for the path with an adjusted waypoint, respectively. It is important to note that these adjustments come from adjusting the waypoint that has been pulled off the optimal path, instead of choosing different combinations of waypoints, like in Table 4 - Table 7.

Table 2 and Table 3 show the accelerations when the waypoint path is adjusted in the x and y direction, respectively. The original acceleration for a path with a waypoint at 25% is 215.8927 and the derivatives directly show how much impact adjusting the waypoint position has. Table 2 indicates that changing the waypoint position in the x direction has more of an impact than changing the waypoint in the y direction, as the derivative is higher for x adjustments. It is also shown that adding to the x position results in a higher derivative than subtracting from the x position. Table 3 shows that the most impact for adjusting a waypoint in the y direction is when it is added, as it results in the highest derivative.

Table 2: Comparison of Total Acceleration for Adjusted X Position for Waypoint Pulled Off Optimal Path

Path Description	Adjustment	Total Acceleration (m/s²)	Derivative
Path with a waypoint at 25%	+1 in the X direction	215.941	0.0486

Path with a waypoint at 25%	-1 in the X direction	215.844	0.0485
Path with a waypoint at 25%	+10 in the X direction	216.380	0.0487
Path with a waypoint at 25%	-10 in the X direction	215.409	0.0484

Table 3: Comparison of Total Acceleration for Adjusted Y Position for Waypoint Pulled Off Optimal Path

Path Description	Adjustment	Total Acceleration (m/s²)	Derivative
Path with a waypoint at 25%	+1 in the Y direction	215.938	0.0459
Path with a waypoint at 25%	-1 in the Y direction	215.846	0.0457
Path with a waypoint at 25%	+10 in the Y direction	216.358	0.0466
Path with a waypoint at 25%	-10 in the Y direction	215.442	0.0450

The results from the second method of trying different combinations of a waypoint not from the optimal path help to show if certain parameters, such as x or y position, have a greater impact on a waypoint's success. These changes are applied to a waypoint time of 50 seconds, as previous calculations showed the lowest total acceleration with a waypoint at 50% of the time of flight, which is 100 seconds. Table 4 - Table 7 show different combinations of x position, y position, x velocity, and y velocity, respectively. Table 4 shows that the value that yields the

lowest total acceleration is when the x position is approximately 500 meters. When it is increased or decreased away from that value, the acceleration increases, especially when decreased.

Table 4: Comparison of Different X Position Values for a Waypoint

X, Y Position (m)	X, Y Velocity (m/s)	Waypoint Time (sec)	Total Acceleration (m/s²)
[-500, 80]	[20, -1]	50	273.8732
[250, 80]	[20, -1]	50	225.0857
[500,80]	[20, -1]	50	221.5494
[1000, 80]	[20, -1]	50	224.2484
[1500, 80]	[20, -1]	50	234.2606

Table 5 shows that the value that yields the lowest total acceleration is when the y position is approximately 500. When it is increased or decreased away from that value, the acceleration increases, especially when increased.

Table 5: Comparison of Different Y Position Values for a Waypoint

X, Y Position (m)	X, Y Velocity (m/s)	Waypoint Time (sec)	Total Acceleration (m/s²)
[500, -500]	[20, -1]	50	238.9957
[500, 30]	[20, -1]	50	222.4239
[500, 120]	[20, -1]	50	220.9472
[500, 500]	[20, -1]	50	220.3222

[500, 1000]	[20, -1]	50	238.2286
[500, 1500]	[20, -1]	50	275.8049

Table 6 shows that the value that yields the lowest total acceleration is when the x velocity is extremely small and close to 0.5 m/s. When it is increased or decreased away from that value, the acceleration increases, especially when increased.

Table 6: Comparison of Different X Velocity Values for a Waypoint

X, Y Position (m)	X, Y Velocity (m/s)	Waypoint Time (sec)	Total Acceleration (m/s²)
[500, 80]	[0.5, -1]	50	205.8236
[500, 80]	[5, -1]	50	208.2240
[500, 80]	[10, -1]	50	211.9543
[500, 80]	[20, -1]	50	221.5494
[500, 80]	[40, -1]	50	246.7542

Table 7 shows that the value that yields the lowest total acceleration is when the y velocity is close to 20 m/s. When it is increased or decreased away from that value, the acceleration increases, especially when increased.

Table 7: Comparison of Different Y Velocity Values for a Waypoint

X, Y Position (m)	X, Y Velocity (m/s)	Waypoint Time (sec)	Total Acceleration (m/s²)
------------------------------	--------------------------------	--------------------------------	---

[500, 80]	[20, -10]	50	230.3498
[500, 80]	[20, -1]	50	221.5494
[500, 80]	[20, 20]	50	208.6634
[500, 80]	[20, 40]	50	211.6704
[500, 80]	[20, 80]	50	258.9972

Another important factor in implementing a waypoint is the switching time. When the path is being calculated with a waypoint, it includes a set amount of time to allow the path to reach the waypoint and then continue along to the target. The effects of changing this switching time are investigated as part of this numerical simulation. Table 8 shows that a local minimum likely exists for a switching time of 4 seconds. However, the difference in lowering the switching time from 5 seconds to 3 seconds is very minimal, while increasing the switching time has more impact on the total acceleration.

Table 8: Comparing Switching Time for a Path with a Waypoint at 50%

Switching Time (sec)	Total Acceleration (m/s²)
3	213.4450
4	213.2629
5	213.6398
7	214.9028
8	215.6168

The following result shows that when lunar gravity is removed from the problem, it is easy to achieve similar total acceleration. However, Chapter 2 mentions that without a uniform

constant gravity vector, that optimality for a ZEM/ZEV method should not be achieved. Figure 13 shows the similarity between the paths, but even more important is the total acceleration. For this case, the total acceleration of the original optimal path is 201.6055 m/s^2 , while the total acceleration for the path with a waypoint at 10% is 201.6275 m/s^2 . These results are almost identical and this should not be the case.

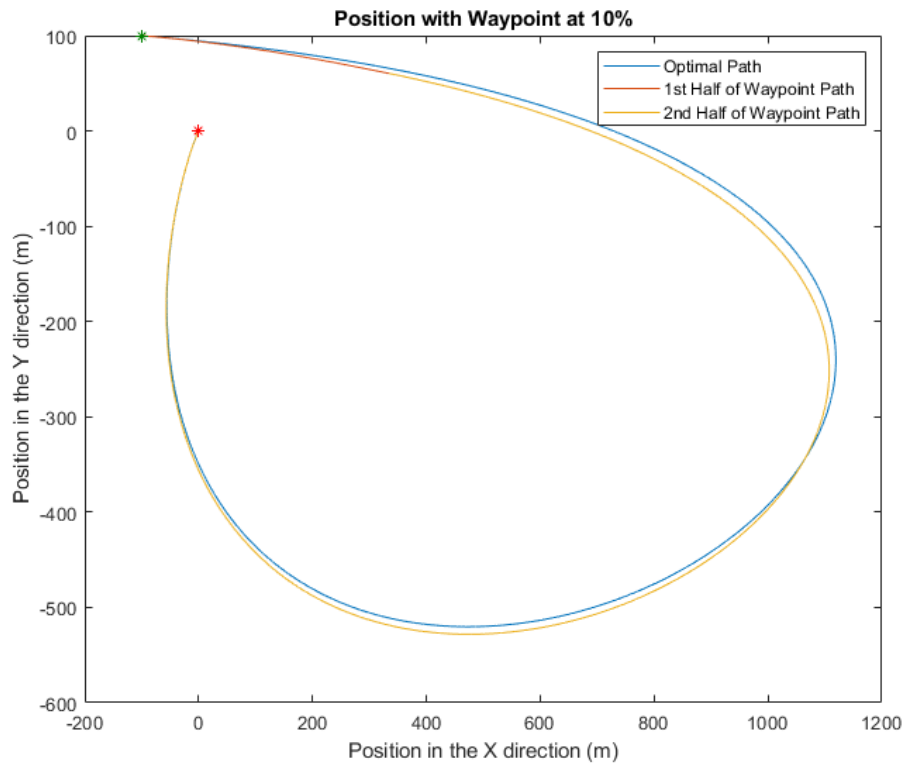


Figure 13: Comparison of Position for Optimal Path and Path with a Waypoint at 10% with No Gravity

Section 4.2 presents results that come from using the genetic algorithm within Matlab. The outcome of the genetic algorithm are waypoint characteristics (x and y position, x and y velocity, and waypoint time). The goal of this section is to compare what the genetic algorithm finds as the optimal waypoint to the results in Section 4.1. To do this, the genetic algorithm characteristics are changed. Characteristics that can be changed are population size, and bounds for position, velocity, and time of flight.

4.2 Genetic Algorithm

A genetic algorithm (GA) is a method for solving an optimization problem that is like the natural selection process. This genetic algorithm is executed in Matlab and at each step, the algorithm selects a result from the population to produce new results for a new generation (Matlab). Through each of these generations, the genetic algorithm reaches an optimal solution. The GA accepts a function that runs the ZEM/ZEV method through the ODE45 and has the same initial and target position and velocities. By setting up the GA this way, the results of the GA are directly compared to the results from the original test driver that runs ODE45 with the ZEM/ZEV method. The derivative is also found. If a derivative is equivalent to zero, it indicates optimality. The equation to find the derivative is Eq. 3.15.

There are different parameters that change when implementing the GA, such as population size and bounds for function inputs. It is better to run a larger population size and Table 9 shows the outcome of different population sizes and the effect it has on the total acceleration and waypoint time. To show the effect of population size, the input bounds in remain constant. The x position ranges from [-2000, 2000] meters, the y position ranges from [-2000, 2000] meters, the x velocity ranges from [0, 100] meters/sec, the y velocity ranges from [-100, 100] meters/sec and the waypoint time ranges from [6, 99] sec. The waypoint time range must start at six seconds because the waypoint switching time is five seconds.

Table 9: Genetic Algorithm Results with Different Population Sizes

Population Size	Generations	Total Acceleration (m/s²)	Waypoint Time (sec)
100	25	193.5	7.31
1,000	21	188	70.84
10,000	13	184.3	36.97

The results in Table 9 are iterated until the fitness of the GA levels out for a given population size, as shown in Figure 14. This means that the number of generations needed to reach a conclusive answer can differ, if there are no spikes in the fitness.

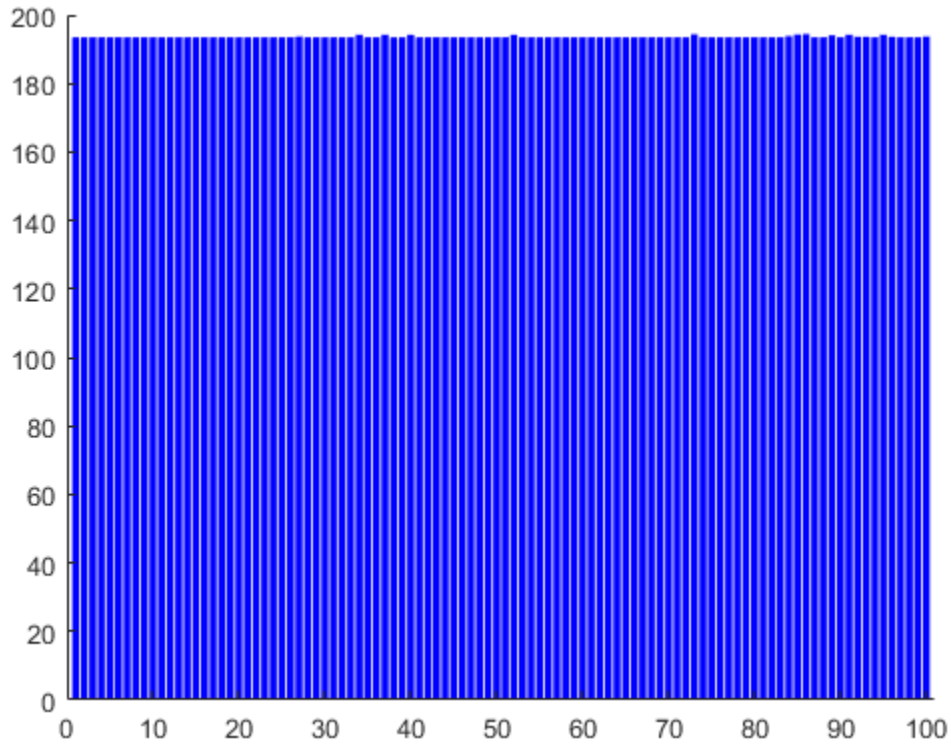


Figure 14: Fitness for GA at Final Generation

When the input bounds for the waypoint time are changed from [6, 99] sec to [20, 99] sec using a population size of 1,000, a similar outcome to the test case using a population size of 10,000 and 13 generations from Table 9 occurs. Figure 15 shows the position for the test case using a population size of 10,000.

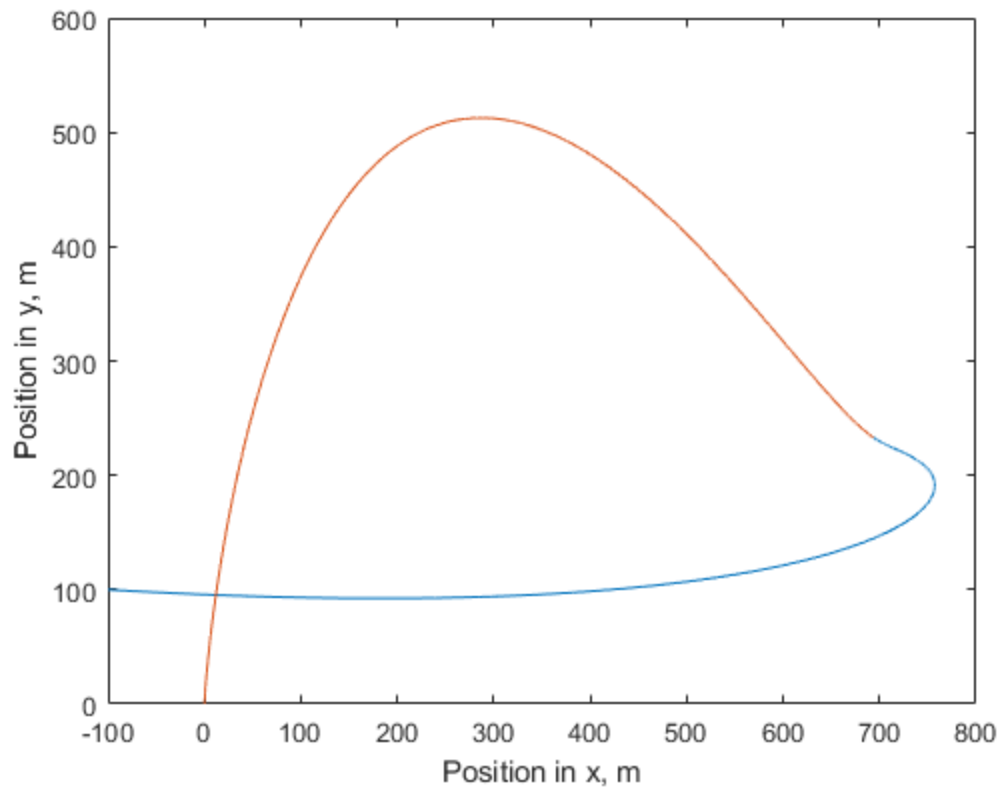


Figure 15: Position in X and Y for Genetic Algorithm (Population Size: 10000, Waypoint range: [6,99] sec)

It only takes 20 iterations using a population size of 1,000 for the fitness to level out and reach a total acceleration of 184.5 m/s^2 with a waypoint time of 38.18 seconds. Figure 16 show the outcome in terms of x and y position.

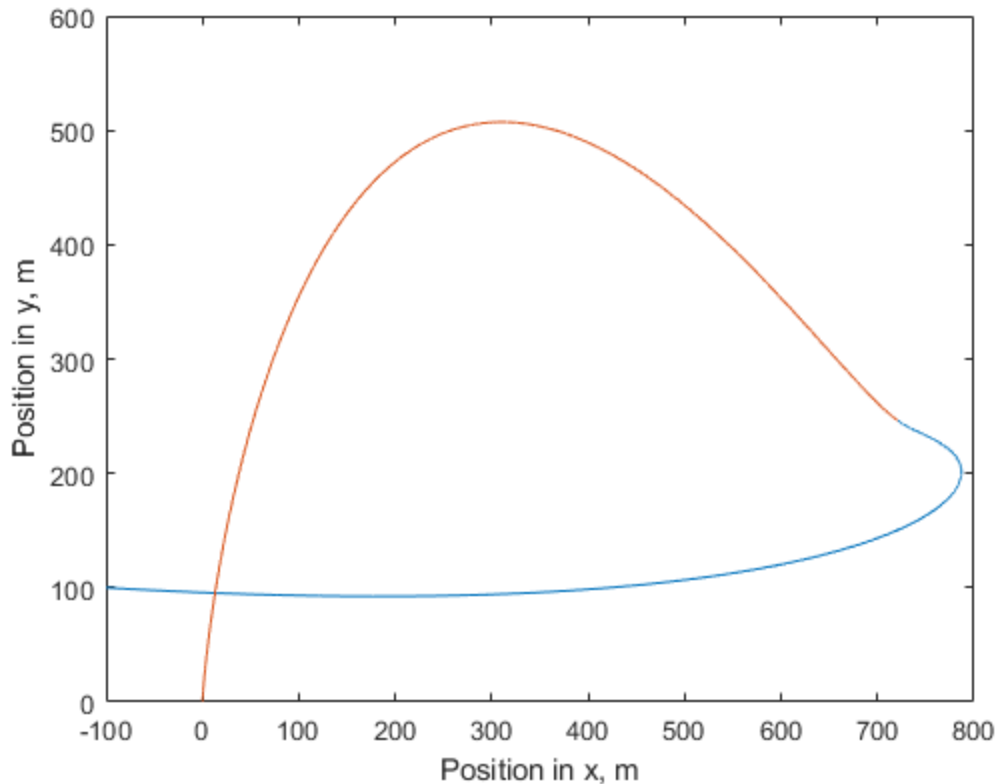


Figure 16: Position in X and Y for Genetic Algorithm (Population Size: 1000, Waypoint range: [20,99] sec)

It is seen that the graph outcome between Figure 15 and Figure 16 have similar trends and values, despite having different waypoint time range and different population sizes. This indicates that the waypoint time range has an impact on results. Changing the waypoint bounds is also explored to see the effects on the outcome.

Table 1 shows the differences in changing waypoint bounds. The position and velocity bounds remain the same throughout each test, as well as the population size. The population size is 1,000, the x and y position bounds are [-2000,2000] meters, the x velocity bound is [0,100] m/sec, and the y velocity bound is [-100,100] m/sec.

Table 10: Effects of Changing Waypoint Bounds for GA

Waypoint Time Bounds (sec)	Total Acceleration Determined (m/s²)	Waypoint Time Determined (sec)
[6,99]	188	70.83
[20,99]	184.5	38.17
[30,99]	184.8	37.60
[50,99]	187.6	76.98

While no result from the GA directly matched the optimal path found only using the ZEM/ZEV method, when the results from the GA are plugged into the ZEM/ZEV method, the same acceleration is achieved. This indicates that the ZEM/ZEV method can achieve the same result, provided it is given the optimized waypoint position, velocity, and time.

Section 4.2 presents results from calculating the L2 norm for all possible waypoints. The goal of this section is to evaluate waypoints using a different metric from the total acceleration.

5 Conclusion

Many different methods are used to explore the characteristics that dictate what makes a waypoint an ideal waypoint. A waypoint consists of x and y position, x and y velocity, and a given time. By comparing different values for these variables, as well as comparing to different optimal solutions, the results help to show what makes a good waypoint for a lunar landing mission. The percentage of the waypoint for a given path is one of the first parameters investigated and shows that when the waypoint is placed at 30% - 50% of the path, it exhibits lower total acceleration and when it is placed toward 80-90% of the path, it exhibits much higher total acceleration, according to Table 1. The reasoning for the waypoint exhibiting lower total acceleration around 30% - 50% is likely due to the switching time, as the having the waypoint be too early along the path does not allow much time for the spacecraft to transition to the waypoint and continue along the path.

Next, the method of choosing different combinations of waypoint, which is not pulled off the optimal path is explored, as presented in Table 4 - Table 7. The arbitrary waypoint choices show that for this case of a lunar landing mission, the waypoint shows less total acceleration when the x position is around 500 meters, the y position around 500 meters, the x velocity around 0.5 m/s and the y velocity around 20 m/s. These values correspond to having a waypoint in the range of approximately 30% - 50% of the path, which further verifies that whether the waypoint is pulled off the optimal path or is chosen arbitrarily, the results are similar.

The switching time is also investigated and shows that while it does have an impact on the total acceleration when tested in the regular ZEM/ZEV method with a waypoint, it is very minimal. Table 8 shows that the total acceleration only varies by up to 2 m/s^2 when the switching

time is varied. When the switching time is decreased, it changes by only one tenth of a m/s^2 and when it is increased, typically changes by 1 m/s^2 .

The results from the genetic algorithm also further verify the waypoint positions and velocities that are found in the earlier tests of running the regular ZEM/ZEV method with different waypoints. However, it is important to note that the genetic algorithm achieves a lower total acceleration, at approximately 184 m/s^2 , while the lowest total acceleration from the ZEM/ZEV method with waypoints is closer to 213 m/s^2 . This discrepancy indicates that the genetic algorithm is calculating waypoint characteristics in a different way than the regular ZEM/ZEV method with a waypoint. However, the waypoint ZEM/ZEV method can output the same path as the genetic algorithm if it is fed those waypoint x and y positions, x and y velocities, and time of waypoint. Not only did the genetic algorithm produce lower total accelerations, but there are also several other path combinations that result in a lower total acceleration than what the original optimal path with the ZEM/ZEV method is achieving. These results show that a path with a waypoint can achieve better results than a path without a waypoint. Evidence provided in this work shows that the ZEM/ZEV approach violates Bellman's principle of optimality because when the path is calculated from the waypoint to the final target, it does not result in the same trajectory for the remaining time. This suggests that the ZEM/ZEV approach, despite being proven as the optimal control law that satisfies the problem, may not have an optimal substructure.

There is also simulation-based evidence that the optimality of the ZEM/ZEV method without a gravity being a constant vector can be achieved and shows issues with statements made from similar research discussed in Chapter 2. Figure 13 shows this when the same total acceleration

can be achieved with the original optimal path and a path with a waypoint at 10% when gravity is not present.

Future work includes developing a functioning algorithm that uses this information to select the best waypoint for a given time increment until the spacecraft has reached its' target. It is important to note that the application is of key importance, and the characteristics that may be important for a planetary landing problem are not necessarily the same for a different application, such as rendezvous.

6 References

- Alvarez Rolins, Armando. *Single Waypoint ZEM/ZEV Based Closed-Loop Controller Design for Rendezvous with a Rotating Target*. M.S. Thesis. Melbourne: Florida Institute of Technology, 2015.
- Ben-Asher, Joseph Z. *Optimal Control Theory with Aerospace Application*. Reston, VA: AIAA, 2010.
- Braun, Robert D. and Robert M. Manning. "Mars Exploration Entry, Descent, and Landing Challenges." *Journal of Spacecraft and Rockets* (2007).
- Bryson, Arthur E. and Yu-Chi Ho. *Applied Optimal Control: Optimization, Estimation, and Control*. New York: Wiley, 1975.
- Chang, Kenneth. *Why Everyone Wants to Go Back to the Moon*. 12 July 2019. Online article.
- D'Souza, Christopher N. "An Optimal Guidance Law for Planetary Landing." *Guidance, Navigation, and Control Conference*. AIAA, 1997.
- Ebrahimi, Behrouz, Mohsen Bahrami and Jafar Roshanian. "Optimal sliding-mode guidance with terminal velocity constraint for fixed-interval propulsive maneuvers." *Acta Astronautica* (2008): 556-562.
- Furfaro, Roberto, Michael L. Cupples and Matthew W. Cribb. "Non-linear Sliding Guidance algorithms for precision lunar landing." *Spaceflight Mechanics 2011 - Advances in the Astronautical Sciences: Proceedings of the 21st AAS/AIAA Space Flight Mechanics Meeting*. New Orleans, LA, 2011. 945-964.
- Goddard, Robert H. *A method of Reaching Extreme Altitudes*. Washington: Smithsonian Institution, 1919.

- Guo, Yanning, Matt Hawkins and Bong Wie. "Applications of Generalized Zero-Effort-Miss/Zero-Effort-Velocity Feedback Guidance Algorithm." *Journal of Guidance, Control, and Dynamics* (2013).
- . "Optimal Feedback Guidance Algorithms for Planetary Landing and Asteroid Intercept." *AAS/AIAA Astrodynamics Specialist Conference*. Girdwood, Alaska: American Astronomical Society, 2011.
- . "Waypoint-Optimized Zero-Effort-Miss/Zero-Effort-Velocity Feedback Guidance for Mars Landing." *Journal of Guidance, Control, and Dynamics* (2013).
- Hawkins, Matthew Jay. *New near-optimal feedback guidance algorithms for space missions*. PhD Thesis. Ames: Iowa State University, 2013.
- Hohmann, Walter. *Die Erreichbarkeit der Himmelskörper*. Munich: R. Oldenbourg, 1925.
- Jones, Andrew. *China's Chang'e 5 Moon Landing Site Finally Has a Name*. 8 July 2021. Online article.
- Klumpp, Allan R. "Apollo Guidance, Navigation, and Control." 1971. *hq.nasa.gov*.
- Lawden, Derek F. "Rocket Trajectory Optimization: 1950-1963." *Journal of Guidance, Control, and Dynamics* (1991): 705-711.
- Matlab. *Matlab Genetic Algorithm Description*. n.d.
- Myers, Steven Lee. *The Moon, Mas and Beyond: China's Ambitious Plans in Space*. 17 June 2021. Online article.
- NASA. *As Artemis Moves Forward, NASA Picks SpaceX to Land Next Americans on Moon*. 16 April 2021. Online article.
- . "The Artemis Plan." 2020. *nasa.gov*. 2021.
- Oberth, Hermann. *Wege zur Raumschiffahrt*. Munich: R. Oldenbourg, 1929.

Sharma, Rajnish, John E Hurtado and Srinivas R Vadali. "Optimal Nonlinear Feedback Control Design Using a Waypoint Method." *Journal of Guidance, Control, and Dynamics* (2011): 698-705.

Singh, Surendra. *Covid curbs delay Chandrayaan-3 mission by one more year; launch likely occurring during third quarter of 2022*. 29 July 2021. Article.

Siouris, George M. *Missile Guidance and Control Systems*. New York: Springer, 2004.

Society, Planetary. *Chang'e-4 and Yutu-2, China's mission to the Moon's far side*. 2019. Online article.

Wie, Bong. *Space Vehicle Guidance, Control, and Astrodynamics*. Reston, VA: AIAA, 2015.